

## Supporting Information

### **Flexible hierarchically PANI/MnO<sub>2</sub> porous network with fast channels and extraordinary chemical process for stable fast-charging lithium-sulfur battery**

Yunjing Zhang,<sup>a,1</sup> Xiaolin Liu,<sup>b, c,1</sup> Liang Wu,<sup>a</sup> Wenda Dong,<sup>a</sup> Fanjie Xia,<sup>a,d</sup> Liangdan Chen,<sup>a</sup> Na Zhou,<sup>a</sup> Lixue Xia,<sup>b,c</sup> Zhi-Yi Hu,<sup>a,d</sup> Jing Liu,<sup>a</sup> Hemdan S. H. Mohamed,<sup>a,e</sup> Yu Li,<sup>a,d\*</sup> Yan Zhao,<sup>b,c\*</sup> Lihua Chen<sup>a</sup> and Bao-Lian Su<sup>a,f\*</sup>

<sup>a</sup> State Key Laboratory of Advanced Technology for Materials Synthesis and Processing, Wuhan University of Technology, 122 Luoshi Road, 430070, Wuhan, Hubei, China.

<sup>b</sup> State Key Laboratory of Silicate Materials for Architectures, Wuhan University of Technology, 122 Luoshi Road, 430070, Wuhan, China

<sup>c</sup> International School of Materials Science and Engineering, Wuhan University of Technology, Wuhan 430070, Wuhan, China

<sup>d</sup> Nanostructure Research Centre (NRC), Wuhan University of Technology, 122 Luoshi Road, 430070 Wuhan, Hubei, China.

<sup>e</sup> Physics Department, Faculty of Science, Fayoum University, El Gomhoria Street, 63514 Fayoum, Egypt

<sup>f</sup> Laboratory of Inorganic Materials Chemistry (CMI), University of Namur, 61 rue de Bruxelles, B-5000 Namur, Belgium.

<sup>1</sup> These two authors contributed equally to this work.

\*Corresponding authors: [yu.li@whut.edu.cn](mailto:yu.li@whut.edu.cn), [yan2000@whut.edu.cn](mailto:yan2000@whut.edu.cn) and [bao-lian.su@unamur.be](mailto:bao-lian.su@unamur.be)

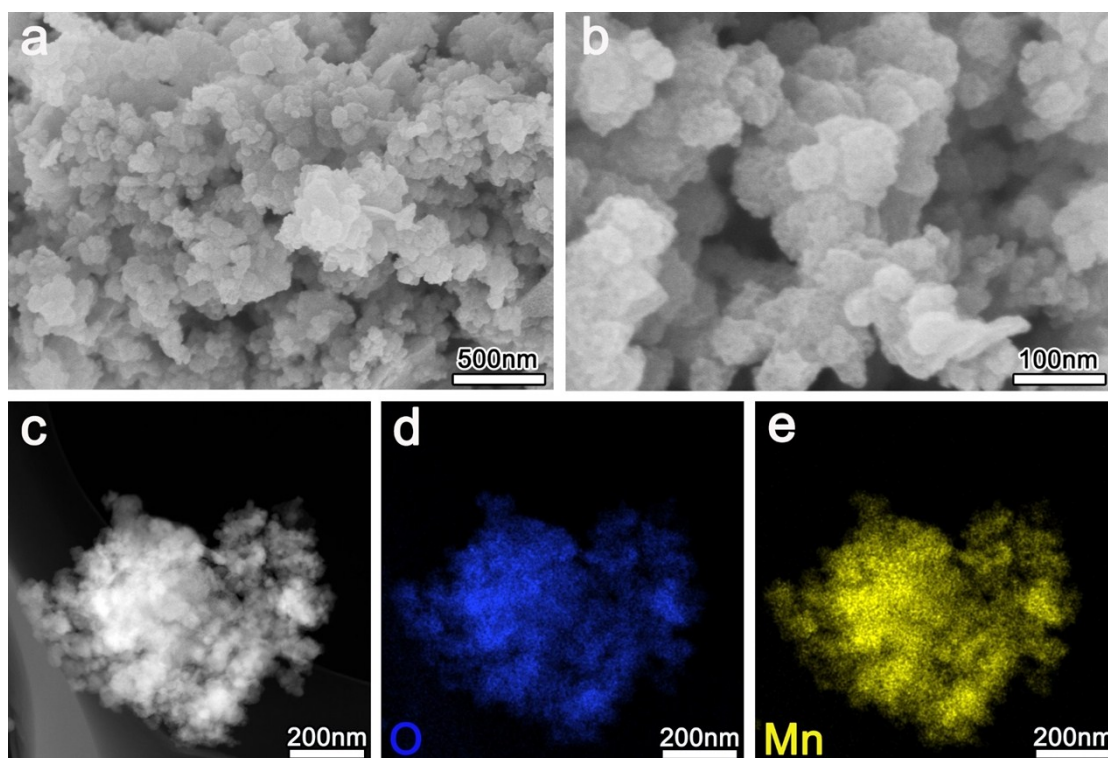


**Figure S1.** (a)-(b) SEM characterization of  $\text{MnO}_2$ ; (c-e) corresponding EDX elemental mapping of the  $\text{MnO}_2$ , O: blue and Mn: yellow.

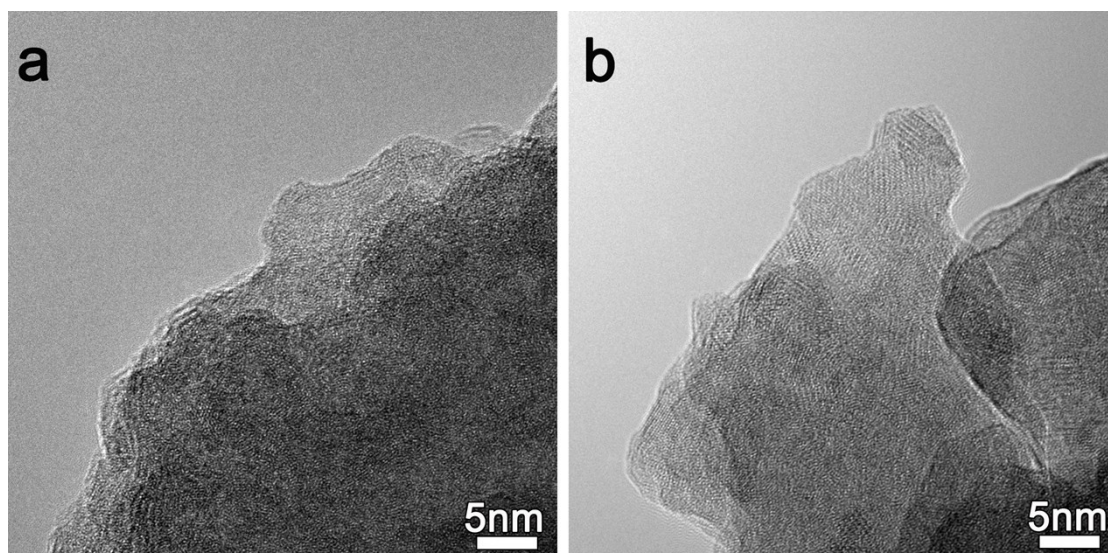


**Figure S2.** HR-TEM image of (a) PANI- $\text{MnO}_2$  and (b)  $\text{MnO}_2$ .

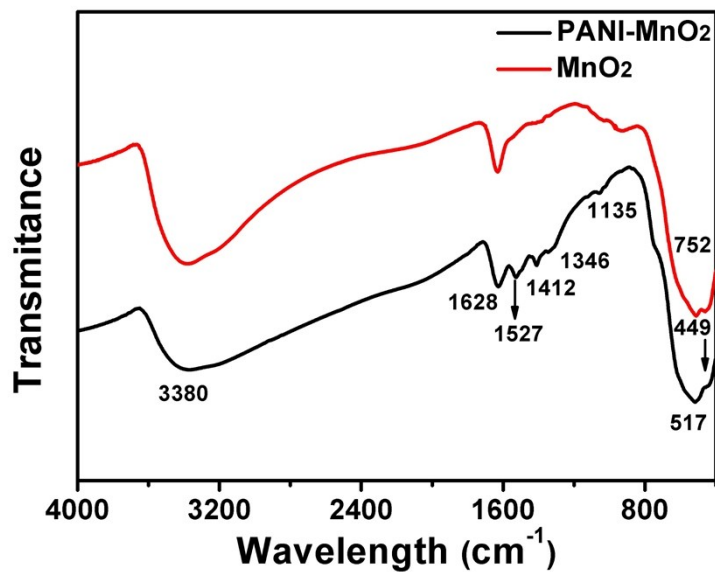


Figure S3. FTIR spectrums of PANI-MnO<sub>2</sub> and MnO<sub>2</sub>.

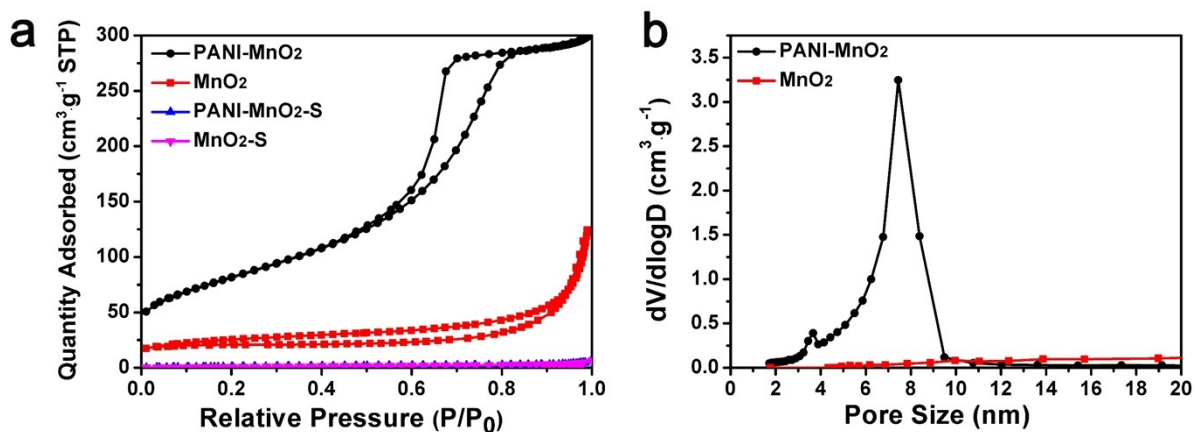


Figure S4. The nitrogen adsorption-desorption isotherms (a) and corresponding pore size (b) distributions of PANI-MnO<sub>2</sub> and MnO<sub>2</sub>.

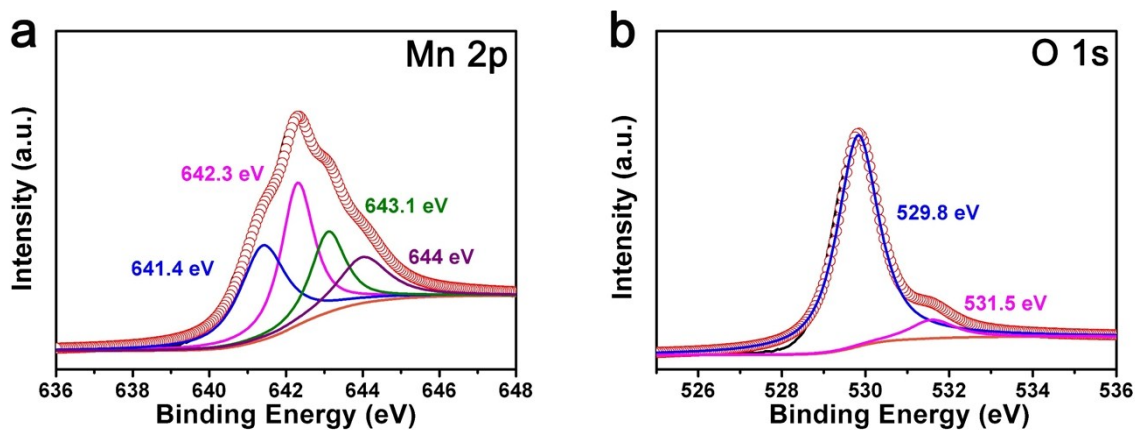
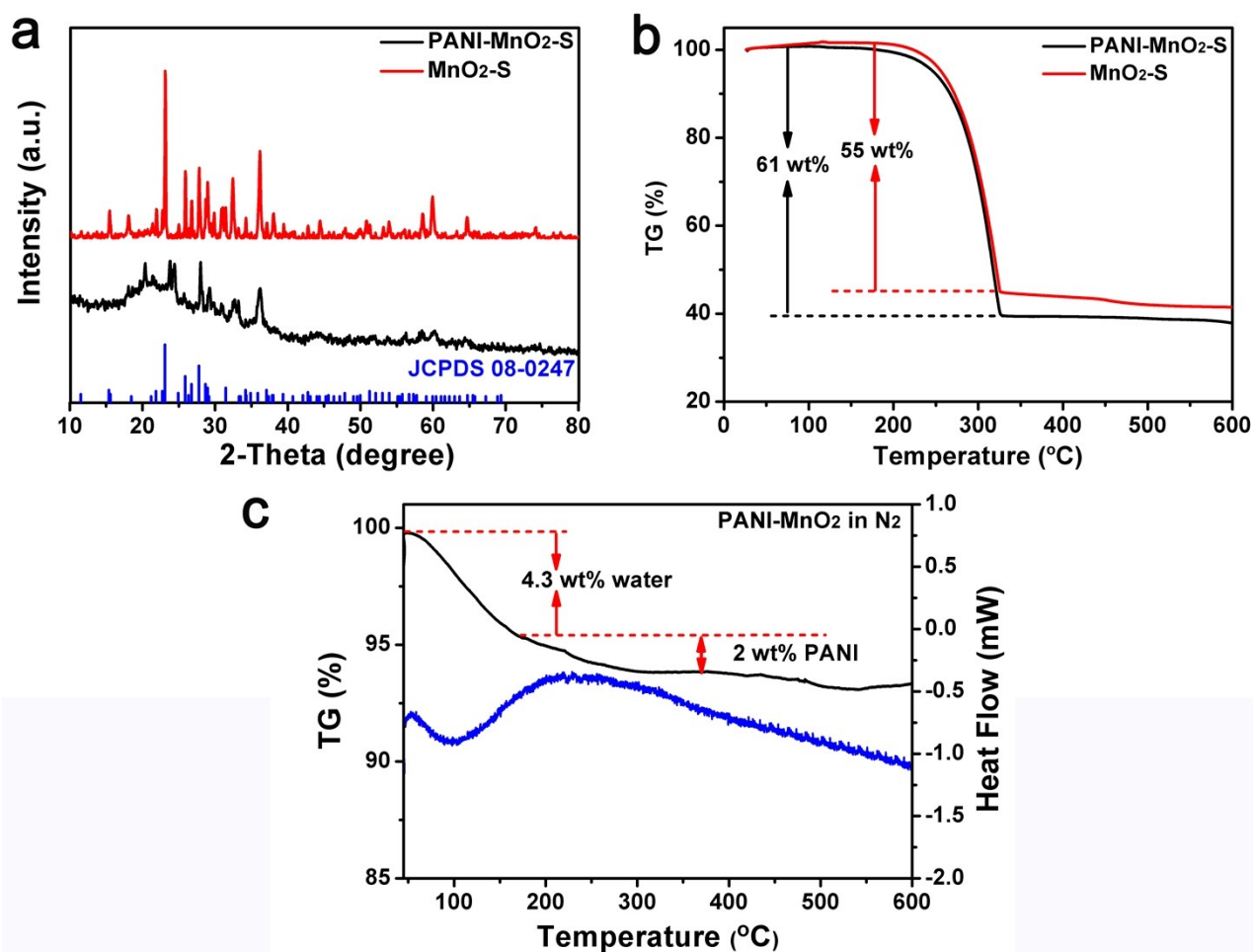
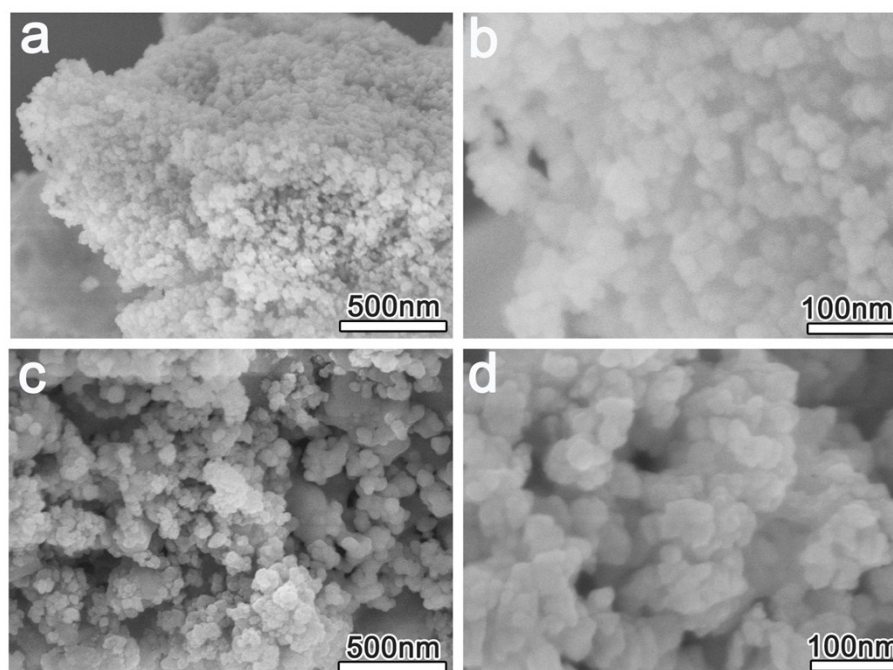


Figure S5. High-resolution Mn 2p<sup>3/2</sup> (a) and O 1s (b) spectrums of MnO<sub>2</sub>.



**Figure S6.** (a) XRD patterns of PANI-MnO<sub>2</sub>-S and MnO<sub>2</sub>-S; (b) TG curve of PANI-MnO<sub>2</sub>-S and MnO<sub>2</sub>-S in N<sub>2</sub>; (c) TG and DSC curve of PANI-MnO<sub>2</sub> in N<sub>2</sub>.



**Figure S7.** SEM characterization of PANI-MnO<sub>2</sub>-S and MnO<sub>2</sub>-S. (a)-(b) PANI-MnO<sub>2</sub>-S; (c)-(d) MnO<sub>2</sub>-S.



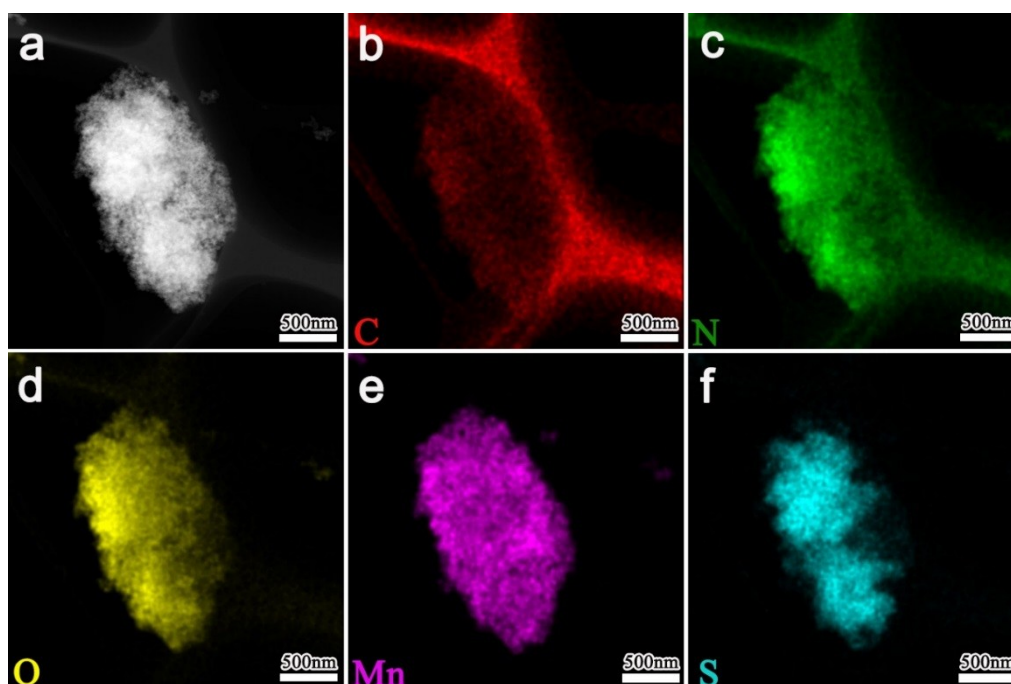


**Figure S8.** A TEM image (a) and the corresponding elemental mappings (b-f) for C, N, O, Mn and S of PANI-MnO<sub>2</sub>-S. C: red; N: green; O: yellow; Mn: purple and S: cyan.

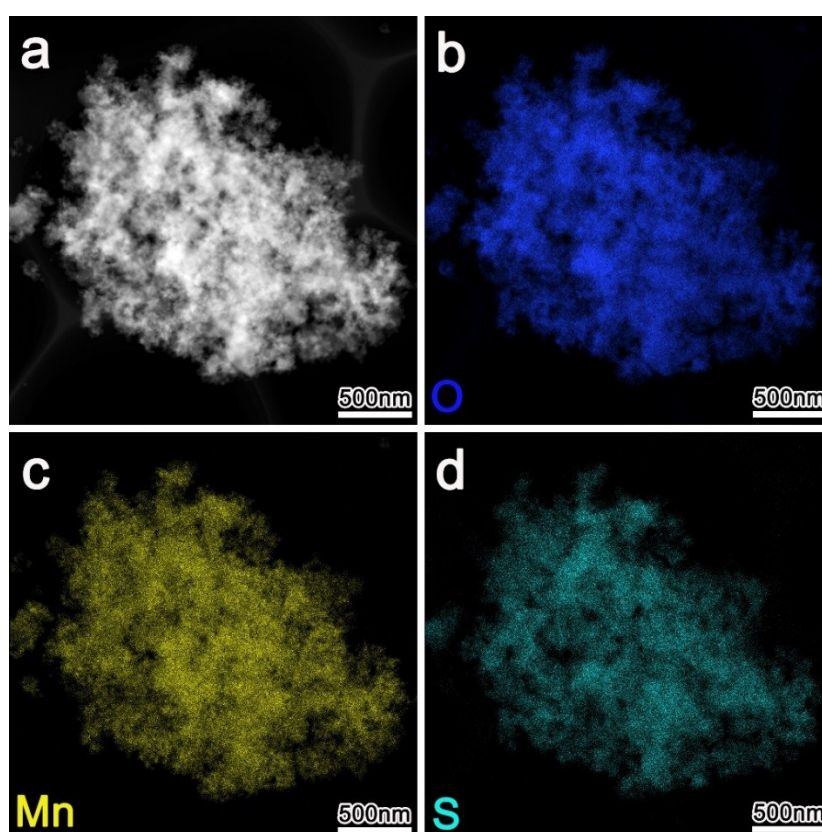


**Figure S9.** A TEM image (a) and the corresponding elemental mappings (b-d) for O, Mn and S of MnO<sub>2</sub>-S. O: blue; Mn: yellow and S: cyan.

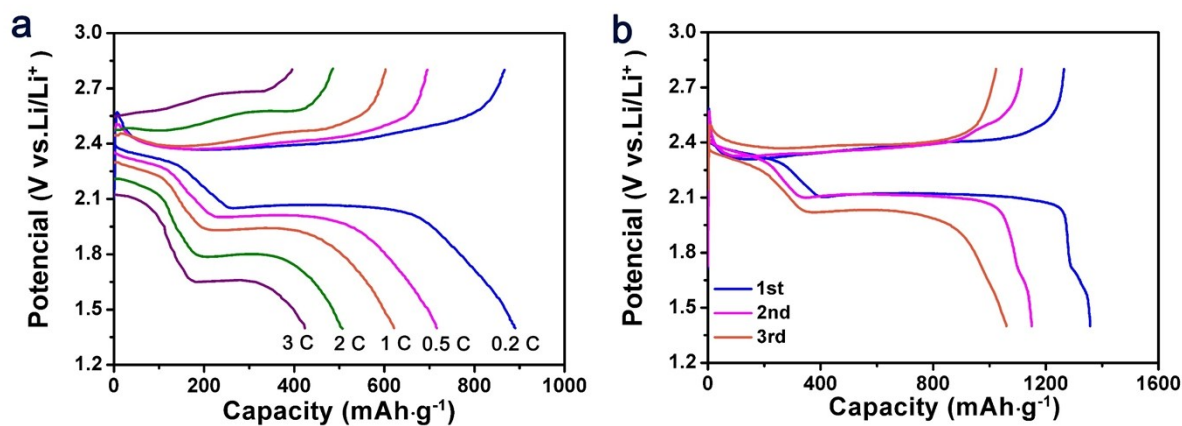


**Figure S10.** (a) Charge-discharge profiles of MnO<sub>2</sub>-S electrode at various rate; (b) the first three cycles of charge-discharge profiles of MnO<sub>2</sub>-S electrode at 0.5 C.

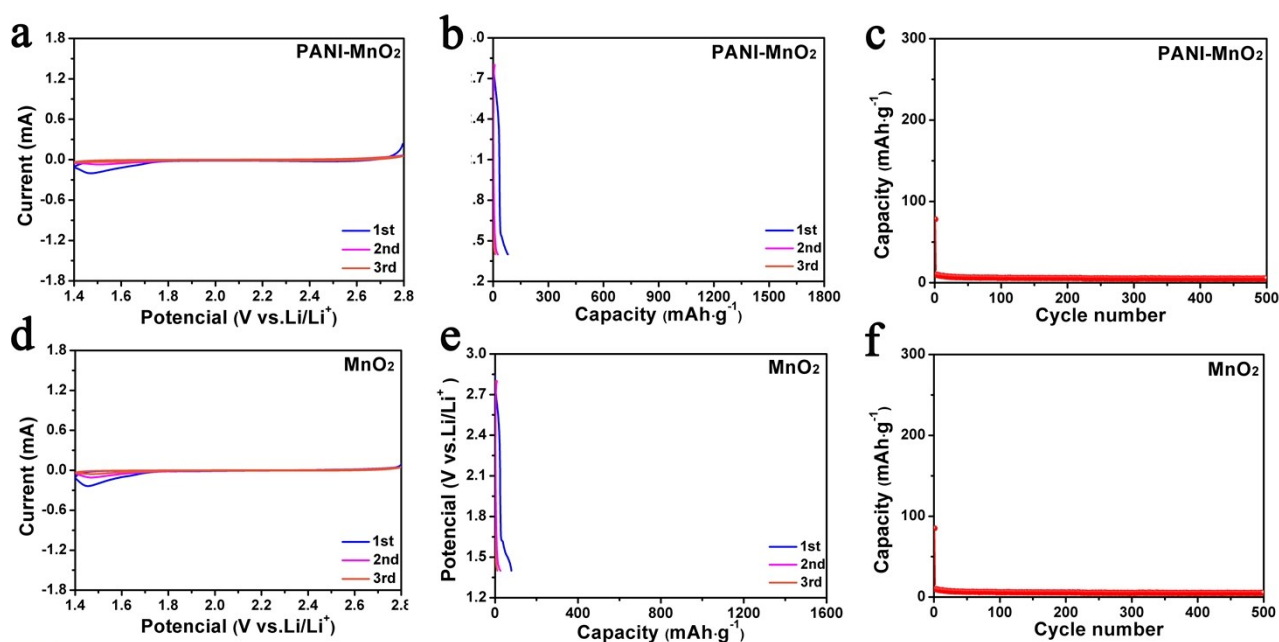


**Figure S11** CV curves of PANI-MnO<sub>2</sub> (a) and MnO<sub>2</sub> (d) electrode at 0.2 mV·s<sup>-1</sup>; the first three cycles of charge/discharge profiles of PANI-MnO<sub>2</sub> (b) and MnO<sub>2</sub> (e) electrode at 0.5 C; the cycle capacity of PANI-MnO<sub>2</sub> (c) and MnO<sub>2</sub> (f) electrode at 0.5 C.

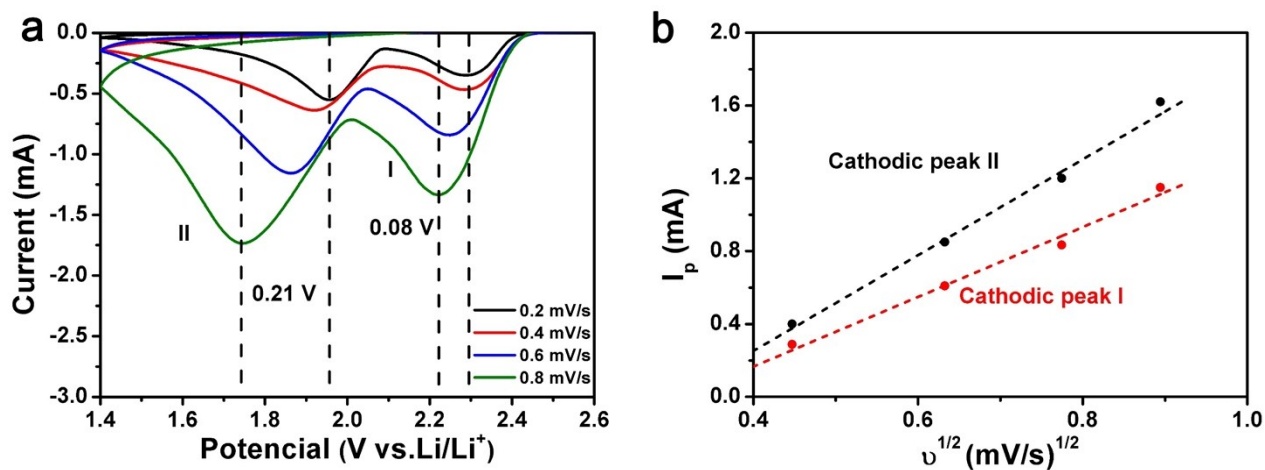


**Figure S12.** (a) CV curves of MnO<sub>2</sub>-S electrode with increase of scan rate from 0.2 to 0.8 mV·s<sup>-1</sup>; (b) the relationship between the peak current  $I_{\text{peak}}$  and the sweep rate  $\nu^{0.5}$  at the two reduction peaks.

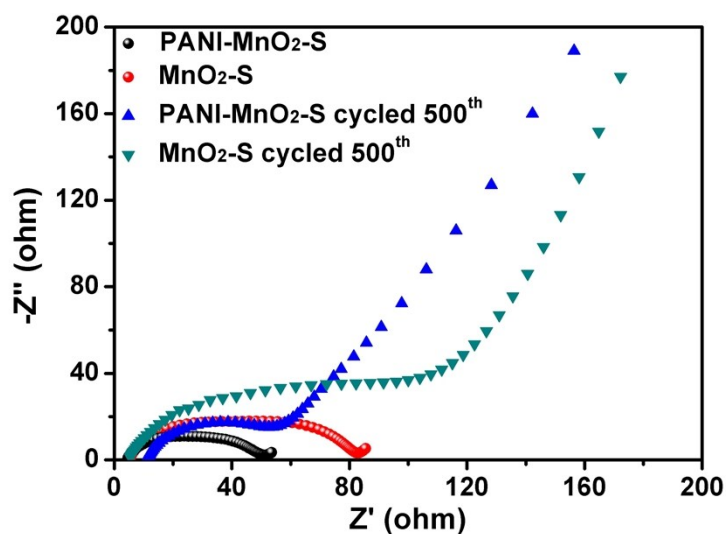


**Figure S13.** Electrochemical impedance spectra (EIS) of PANI-MnO<sub>2</sub>-S and MnO<sub>2</sub>-S cathodes before and after 500 cycles at 2 C.

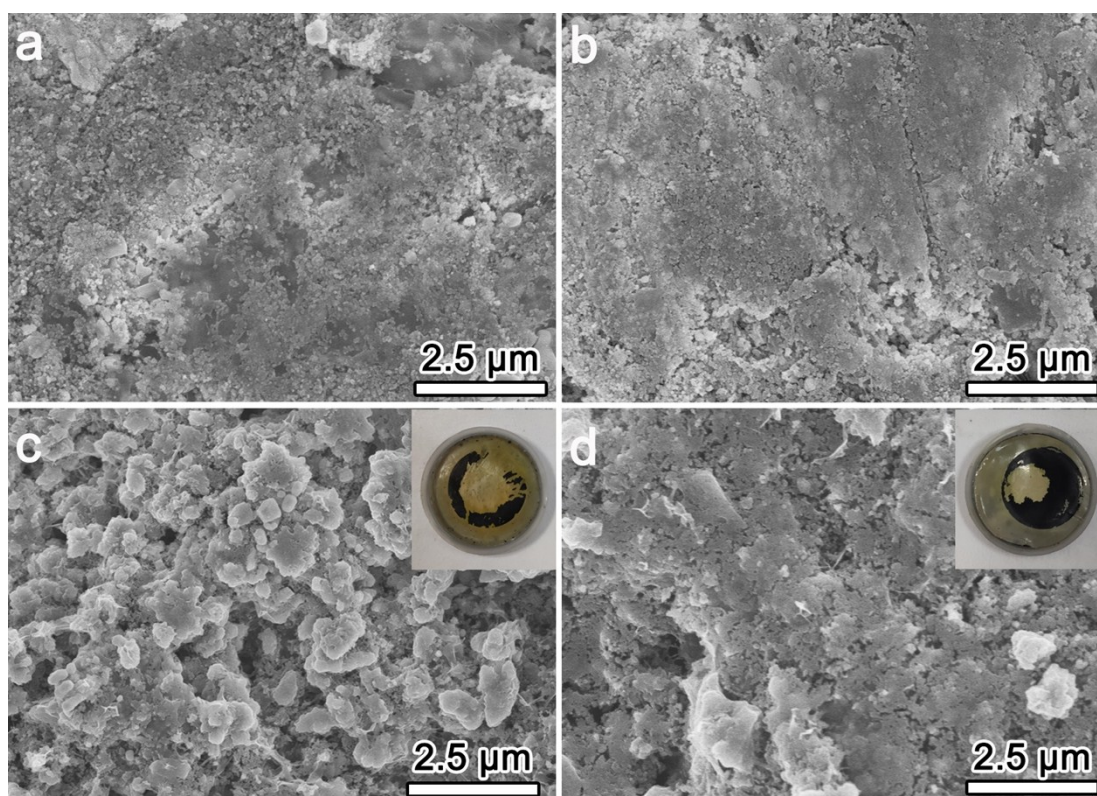


**Figure S14.** The SEM characterization of fresh/cycled electrodes: MnO<sub>2</sub>-S (a) and PANI-MnO<sub>2</sub>-S (b) fresh electrodes; MnO<sub>2</sub>-S (c) and PANI-MnO<sub>2</sub>-S (d) electrodes after 500 cycles at 2 C, Inset: photograph of the corresponding separator.

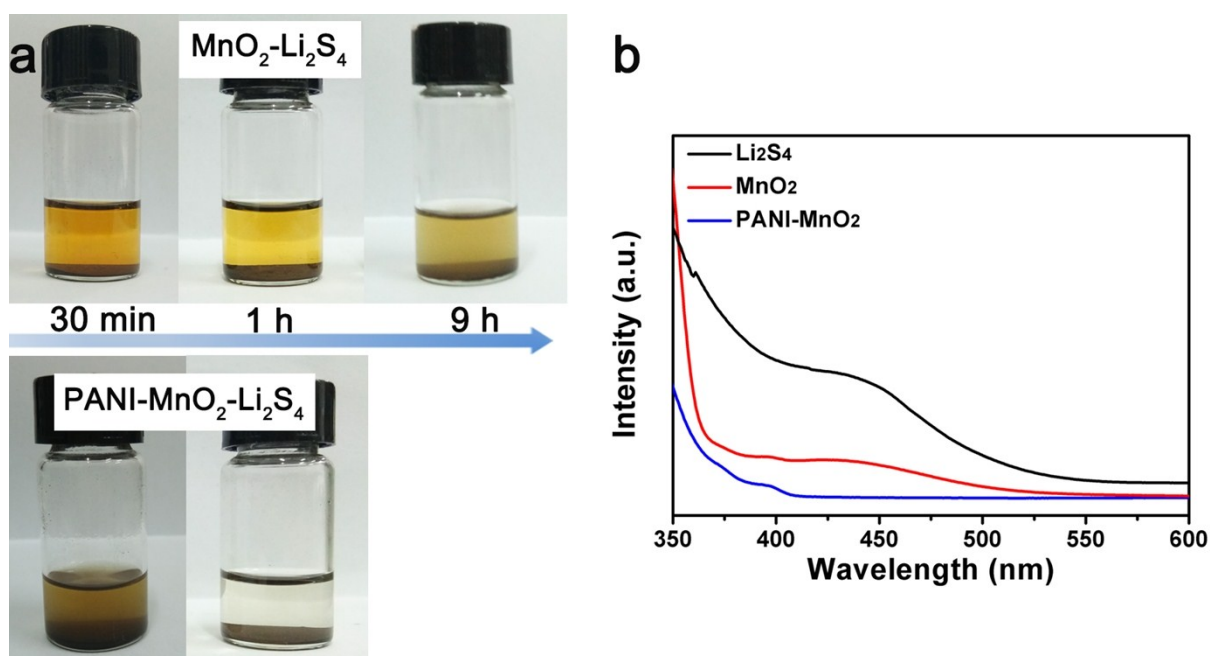


**Figure S15.** (a) Optical pictures of adsorption tests with MnO<sub>2</sub> and PANI-MnO<sub>2</sub> in lithium polysulfides solution (Li<sub>2</sub>S<sub>4</sub> dissolved in DOL/DME solvents, 10 mM); (b) UV-vis spectra (350-600 nm) of the 10 mM Li<sub>2</sub>S<sub>4</sub> solution after exposure with blank, MnO<sub>2</sub> and PANI-MnO<sub>2</sub> composites.



**Table S1** Comparison with previously reported manganese dioxide based carbonaceous host material.

Host materials*	Rate	Cycles	Reversible Capacity (mA h/g)	Ref.
MnO <sub>2</sub> @HCF/S	0.5 C	100	850	21
PPy@MnO <sub>2</sub>	0.5 C	100	720	33
MnO <sub>2</sub> nanosheets-S	0.2 C	200	1030	20
MnO <sub>2</sub> @NHCSs-S	0.5 C	100	860	14
In-situ S@MnO <sub>2</sub>	0.5 C	100	912	22
MnO <sub>2</sub> @HCB/S	1 A/g	60	500	30
S@MnO <sub>2</sub> @GO	0.35 C	50	350	10
S@MnO <sub>2</sub> -C	0.1 C	50	500	61
S@PEDOT/MnO <sub>2</sub>	0.5 C	200	545	31
<b>Mesopore PANI-MnO<sub>2</sub> particles</b>	<b>0.5 C</b>	<b>100</b>	<b>1161</b>	<b>This work</b>

\*HCF: hollow carbon nanofibers; NHCSs: N-doped hollow porous carbon nanospheres; HCB: hollow carbon nanoboxes.